

# Interacting Circular Nanomagnets

A. A. Fraerman, S. A. Gusev, L. A. Mazo, I. M. Nefedov, Yu. N. Nozdrin, I. R. Karetnikova, M. V. Sapozhnikov, I. A. Shereshevskii, L. V. Sukhodoev

Russian Academy of Science

Institute for Physics of Microstructures

GSP-105, Nizhny Novgorod, 603600, Russia

E-mail: msap@ipm.sci-nnov.ru

## Abstract

Regular 2D rectangular lattices of permalloy nanoparticles (40 nm in diameter) were prepared by the method of the electron lithography. The magnetization curves were studied by differential Hall magnetometry for different external field orientations at 4.2K and 77K. The shape of hysteresis curves indicates that there is magnetostatic interaction between the particles. The main peculiarity of the system is the existence of remanent magnetization perpendicular to easy plain. By numerical simulation it is shown, that the feature of the magnetization reversal is a result of the interplay of the interparticle interaction and the magnetization distribution within the particles (vortex or uniform).

PACS: 75.60.Jp

# 1 Introduction

Now it is well known that competition between magnetostatic and exchange energy in a very small ( $\sim 20$  nm) particle leads to a single - domain state. If the radius of a particle is sufficiently large, nonuniform distribution of magnetization has minimal energy. It is a vortex in isotropic magnetic disk. Such particle was referred to as circular nanomagnet [1]. In the case of the individual nanoparticle the vortex has perpendicularly magnetized core [2]. Nowadays the vortex distribution of magnetization in nanomagnets is under detailed investigation [3]. Such systems are considered as perspective for use in RAM (Random Access Memory) device [4]. It is obvious that distribution of magnetization in nanomagnets depends on the interaction between particles. The fundamental type of interaction, which can lead to the long-range ordering [5] and to collective behavior in the system of particles, is the magnetostatic interaction. On the other hand, the energy and a character of the magnetostatic interaction is determined by the magnetization state of the particles.

In this work we experimentally investigate magnetization curves of regular rectangular lattices of permalloy nanoparticles for different external field orientations. We demonstrate that the magnetization distribution within single particle depends on the magnetization process and external field orientation to the lattice axis. It is a result of the interplay of the interparticle interaction and the single particle state. The particles can be both at single-domain and vortex state at zero field. The appearance of the magnetization vortices leads to the appearance of the remanent perpendicular magnetization while magnetizing perpendicular to the easy axis of the system. The competition between the single-domain and vortex states in the system of two magnetostatically interacted magnetic nanodisks has been numerically studied.

## 2 Experiment

Arrays of magnetic particles were fabricated by the electron-beam lithography. The main feature of our method is the usage of fullerene as a resist for electron lithography. Small sizes of  $C_{60}$  molecules and the ability of fullerene to modify its physical and chemical properties under exposure of electrons allow to use this material for a high-resolution nanofabrication. The capabilities of  $C_{60}$  as a negative e-resist have been recently demonstrated by fabrication of 20-30 nm Si pillars [6]. The main steps of the procedure of manufacturing permalloy nanoparticles are thin films deposition, exposing by e-beam, development and two-stage etching. We used a double-layer mask containing the  $C_{60}$  film as a sensitive layer and Ti film as a transmitting layer. Permalloy and Ti films were prepared by pulse laser evaporation on the substrate at room temperature. Fullerene films were deposited by sublimating of a  $C_{60}$  powder at temperature of 350 C in a vertical reactor with hot walls and cooling holder for the substrate. Transmission electron microscopy, selected area diffraction and X-ray diffraction of the metal and fullerene films were carried out to check the crystalline structure and the thickness of layers. Maximum sizes of the metal crystallites did not exceed 5 nm. The  $C_{60}$  films have an amorphous structure. The thickness of the magnetic layers was varied from 25 to 45 nm. The thickness of the masking films was 20 nm for the  $C_{60}$  layer and 30 nm for the Ti film.

The fullerene was patterned in the JEM-2000EX electron microscope with a scanning electron microscopy (SEM) mode by 200 kV e-beam. we had possibility to change the e-beam diameter from 10 nm and over. Utilizing of the high-energy electron beam decreases the amount of backscattering electrons and the shape of patterns becomes defined better. The doses of electron beam irradiation were 0.05-0.1 C/cm<sup>2</sup>, because it assures the reproducibility and uniformity of patterns sizes.

Electron beam irradiation of  $C_{60}$  films reduces the solvability of fullerene in organic solvents. The most likely reason of the changes of the solvability is electron induced polymerization of  $C_{60}$  molecules accompanied by partially graphitization [6, 7]. The exposed samples were developed in the toluene during 1 min and then patterns were transferred to the Ti layer by the plasma etching with  $CF_2Cl_2$  atmosphere. The last step of the fabrication of the magnetic particles was the  $Ar^+$  ion milling of permalloy films using this double-layered mask. Basically, the resistance of the  $C_{60}$  films to the ion milling is sufficient to use this single mask with little bit greater thickness, but the double etch steps are necessary to ensure a uniformity and reproducibility of the sizes of the particles. By carefully monitoring the elemental composition of the samples by means of EDS (energy dispersion spectroscopy), qualitative microanalysis and checking up the morphology of particles by SEM we can better detect the final points of the plasma etching and ion milling processes. However, usually we did some overmilling at the last step, to prevent presence of any magnetic substance between the prepared particles. One of the SEM images of the arrays of the ferromagnetic particles is presented at Fig.1. The shape of the ferromagnetic particles is a disc, which height equals the thickness of the initial permalloy film.

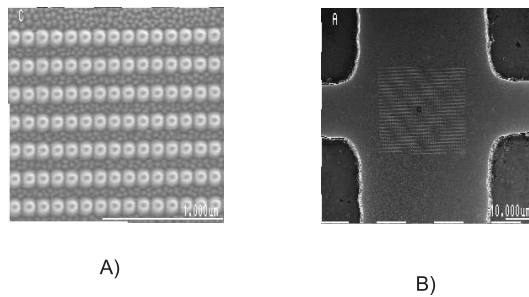


Figure 1: The SEM-image of the sample 1 (See the Table). A) The lattice of the 40-50 nm particles is visible with the background of the 10 nm roughnesses of the sublayer. B) The sample position in the Hall cross.

The parameters of the investigated samples are summarized in the Table. The

symbols  $a$  and  $b$  denote the rectangular lattice parameters (the distances between the centers of the particles),  $h$  is the height of the particles and  $d$  is their diameter. The total number of the particles is equal to  $10^5$ .

Table				
N	a(nm)	b(nm)	h(nm)	d(nm)
1	90	180	45	50
2	120	240	25	80

To carry out measurements of the magnetic properties we choose a differential Hall microsensor technique. Recently it was shown that Hall magnetometer is a very powerful tool for investigation of magnetic properties of 2D nanoparticles lattices [8]. In our work we applied a commercial magnetometer based on the Hall response in a semiconductor (InSb) to investigate a collective behavior of the fabricated 2D permalloy nanoparticle arrays. The widths of the current and the voltage probes are  $100\mu\text{m}$  and  $50\mu\text{m}$  respectively and the thickness of the semiconductor layer is  $10\mu\text{m}$ . The differential magnetometer consisted of two Hall crosses with series connection of the voltage probes. The lattice of the particles was produced in the active area of one of the Hall crosses. The difference in the Hall voltage between this sample cross and the closely spaced empty cross is measured using the bridge circuit [8]. If the bridge is properly balanced, the resulting output voltage is proportional to the sample contribution to the perpendicular component of the magnetic field induction. The large Hall response in the combination with the good coupling

of the small samples to the device results in the excellent spin sensitivity (ratio signal/noise is approximately 100). The sensor works over a large range of the magnetic field and temperature. We have investigated the magnetic properties of the samples by measuring the perpendicular magnetization as a function of the direction and magnitude of the applied field. We have carried out the investigation for three orientations of the external magnetic field: 1) the field is perpendicular to the sample plane (The polar angle  $\theta = 0^\circ$ ); 2) the field is directed at  $45^\circ$  to the sample plane along the short side of the rectangle cell ( $\theta = 45^\circ$ , the azimuthal angle  $\phi = 0^\circ$ ); 3) the field is directed at  $45^\circ$  to the sample plane along the long side of the rectangle cell ( $\theta = 45^\circ$ ,  $\phi = 90^\circ$ ). The direction  $\phi = 0^\circ$  corresponds to the direction along the chains formed by the particles. The chains are elongated along the short side of the elementary rectangle (Fig. 1A). The experimental results for the first sample for  $T = 4.2K$  are represented on the Figs. 2, 3, 4.

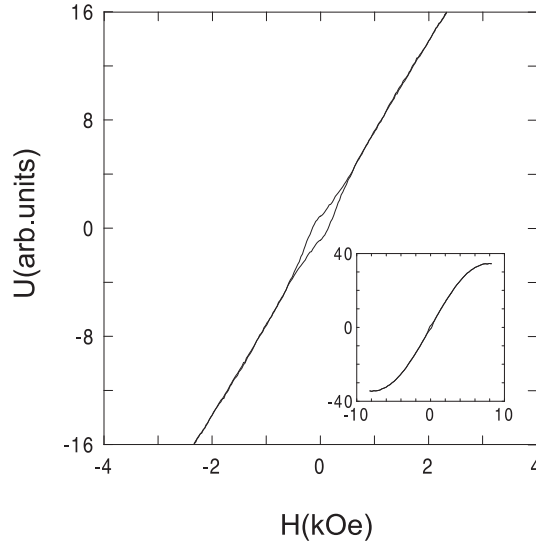


Figure 2: The dependence of Hall signal on the magnetic field with  $\theta = 0^\circ$ . The whole magnetization curve is shown on the casing-in.

The difference of the magnetization curves indicates the collective behavior of the

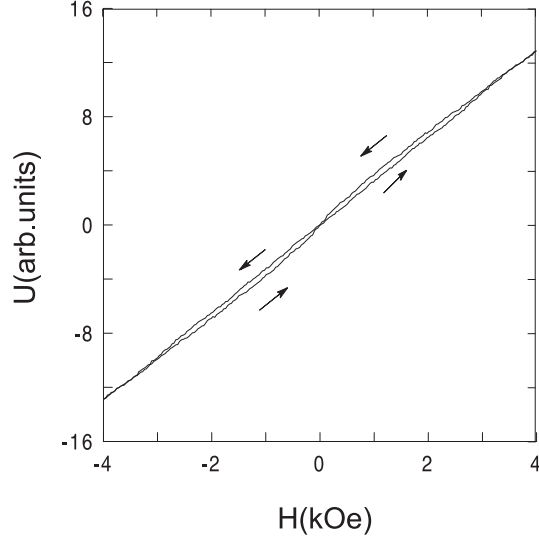


Figure 3: The dependence of the Hall signal on the magnetic field with  $\theta = 45^\circ$ ,  $\phi = 0^\circ$ .

system. It is a result of the magnetostatic interaction between the particles. The hysteresis if the field is directed at  $\theta = 45^\circ$ ,  $\phi = 0^\circ$  (Fig. 3) is the attribute of the easy axis of the magnetization which is directed along the short side of the rectangle cell. The perpendicular remanent magnetization is absent in this case. The existence of such anisotropy in the dipole system was discussed [9, 10]. The magnetization curves if the field is directed at  $\theta = 0^\circ$  or  $\theta = 45^\circ$ ,  $\phi = 90^\circ$  (Figs. 2, 4) are qualitatively similar. They have hysteresis in the weak magnetic field with the remanent magnetization. Remanent magnetization is approximately 5 % of the saturation magnetization. The magnetization curves for the second sample are qualitatively similar to those of the first sample, although the samples have the different shape of the particles (See Table). The particles have the polycrystal structure (this was determined by the X-ray diffraction) and do not have the anisotropy of the form in the plane of the system. In this case the difference of the magnetization curves for the different orientation of the external magnetic field with respect to the sample points to the collective behavior of the particles. The existence of the anisotropy

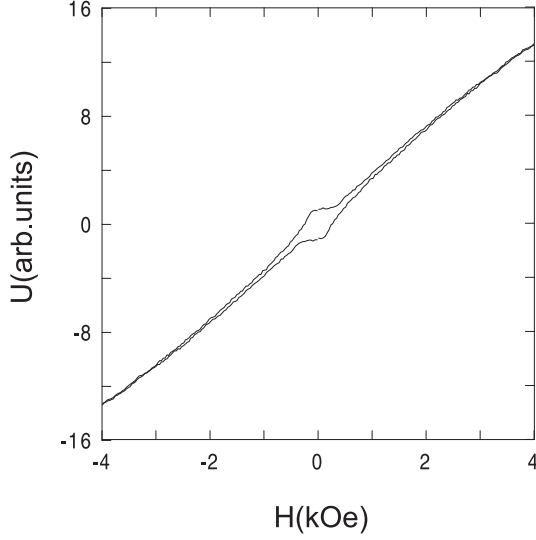


Figure 4: The dependence of the Hall signal on the magnetic field with  $\theta = 45^\circ$ ,  $\phi = 90^\circ$ .

axis in the plane of the rectangular lattice was discussed earlier [9, 10] and was expected. As for the hysteresis and the remanent magnetization for the sample with the rectangular lattice if the external magnetic field direction is  $\theta = 0^\circ$  or  $\theta = 45^\circ$ ,  $\phi = 90^\circ$ , their existence seems to be unexpected. The effect can not be explained by the properties of single particle. Really, for noninteracting particles the remanent magnetization does not depend on a direction of the external magnetic field.

The first sample was also investigated at  $T=77\text{K}$ . The hysteresis if the field was directed at  $\theta = 45^\circ$ ,  $\phi = 0^\circ$  did not be observed. The hysteresis if the field was directed at  $\theta = 0^\circ$  or  $\theta = 45^\circ$ ,  $\phi = 90^\circ$  was qualitatively changed (Fig. 5).

We suppose that the observed behavior of the system is connected with the fact that the particles of the examined sizes can be in two states. First one is a single domain state, the second one is a vortex distribution of the magnetization. In the last case the core of the vortex is magnetized perpendicularly [2]. The interplay of the lattice anisotropy and the anisotropy of dipole interaction between particles leads to the following behavior of the system. The particles turn to be in the sin-



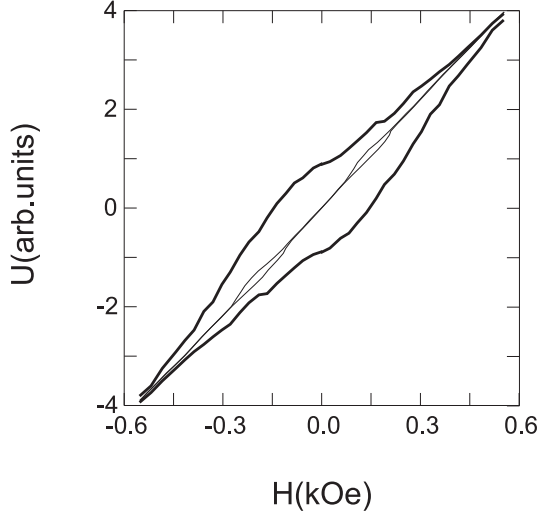


Figure 5: The changing of the magnetization curve hysteresis with the temperature: the thick line for  $4.2^{\circ}K$ , the thin one for  $77^{\circ}K$ .  $H$  is directed at  $\theta = 0^{\circ}$ .

gle domain state if the external field has the component directed along the particle chains. In this case the interaction within chain has the ferromagnetic character and therefore stabilizes the single domain state. On the other hand, if the system is demagnetized within the field perpendicular to the chains the dipole interaction has antiferromagnetic character within the chain and the particles turn to be in the vortex state. As core magnetization has its own coercivity, all cores are ferromagnetically ordered and the system has the remanent perpendicular magnetization. We performed numerical simulation to approve these suggestions.

### 3 Numerical simulation

Let us consider two magnetostatically interacting nanoparticles. This model allows to investigate the magnetization distribution within a particle in the anisotropic system with interaction. We numerically solved the system of stochastic Landau-Lifshitz equations. The effective magnetic field takes in consideration the following components: the applied external magnetic field, the demagnetization field of the

system, the field of anisotropy, is the exchange field within a particle and the random field defined by the thermal fluctuations. The explicit Euler method was used to solve such stochastic differential equation. Note that such an approach to solve stochastic LLH equation is well known and widely used in magnetic simulation [11, 12]. Besides we have used the approximation of uniform distribution of the magnetization in the perpendicular direction. Our numerical scheme is represented in detail in our article [13].

Let us now discuss some results of numerical experiments. First of all, for single magnetic disk we found that the vortex magnetization state becomes ground state only when the height and radius of disk exceeded some critical values. This fact was pointed out earlier in [14] for the square-shape particles. Fig. 6 demonstrates an example of vortex state in cylindrical particle of diameter 50nm and height 12.5nm at zero external magnetic field. Note that such state has nonzero perpendicular component of magnetic moment. This can lead to appearance of hysteresis loop in magnetization curve in systems of magnetic particles.

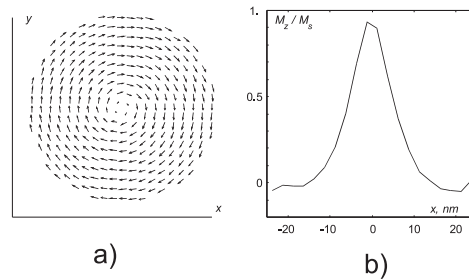


Figure 6: a) The vortex distribution of the magnetization in cylindrical particle. b) the value perpendicular component of the magnetic moment.

If there are two interacting particles, the magnetization curve is changed. Two different cases were considered: first, when the projection of the external magnetic field on disk plane lies along the pair of the particles (it corresponds to  $\theta = 45^\circ$ ,

$\phi = 0^\circ$  in experiment), and second, when this projection lies perpendicularly to pair (it corresponds to  $\theta = 45^\circ$ ,  $\phi = 90^\circ$  in experiment). Diameter of the particle was 50nm, its height was 18nm, the distance between the particle centers was 50nm. The corresponding curves for the perpendicular magnetization are shown in Fig. 7. The hysteresis loop (stars in Fig. 7) is the result of vortex penetrating into the particles at some value of the applied field. In contrast with this situation, the magnetization state remains single-domain at all values of external field when its projection lies along the pair of the particles, and as a result, the curve for perpendicular magnetization has no a hysteresis loop (Fig. 8).

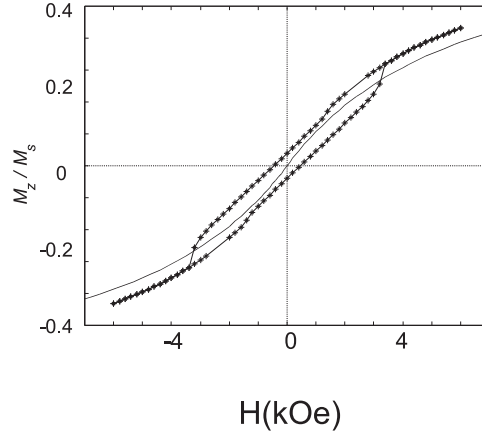


Figure 7: Perpendicular component of magnetization in two particles systems at  $T=4K$ , when external field is applied along the pair of the particles (solid line) and perpendicular to this direction (stars). Angle between external field and the disc is  $45^\circ$ .

## 4 Discussion

The following mechanism for the appearance of the remanent magnetization implies from the results of experimental and numerical simulation suggest with the external field orientation perpendicular to the particle chain. If the external magnetic field has component parallel to the chains, the magnetostatic interaction between

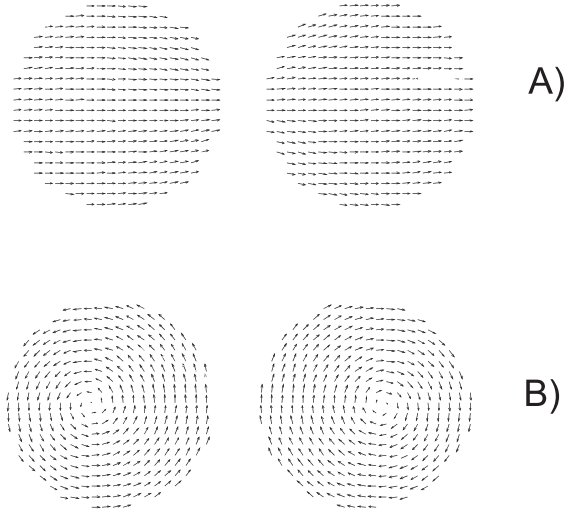


Figure 8: The uniform (A) and vortex (B) magnetization distribution in pair of the permalloy discs.

particles decreases the total energy of the system and the remanent ( $H = 0$ ) state is uniform and the perpendicular component of magnetic moment is absent. In the case when the external magnetic field is perpendicular to the chains, magnetostatic interaction increases the total energy of the system. In order to decrease the energy of the magnetostatic interaction, distribution of the magnetization of the particle takes the vortex form. As discussed earlier, a particle in the vortex state has a nonzero magnitude of the remanent perpendicular magnetization.

Besides there were fundamental changes in the magnetization curve of the sample observed when the sample temperature was raised to 77K (Fig. 5). It points to the fact that thermal fluctuations play a significant role in the system behavior, in spite of  $T_c$  of bulk permalloy is 885K. It is possible that the absence of the remanent magnetization at 77 K is caused by thermally - induced switching between the vortex states with different polarization [15]. If the coercivity of the vortex core become less than the antiferromagnetic magnetostatic interaction between cores the remanent

magnetization of the system will be equal to zero. This hypothesis requires further theoretical investigation.

So it is shown that the interaction in the regular 2D rectangular lattice of nanoparticles plays a significant role. The interplay of anisotropy of magnetostatic interaction and lattice anisotropy determines the magnetization state of the particles. It can be both vortex and single-domain state. Due to possibility of the vortex state existence, the system can have the remanent magnetization directed perpendicularly to the system plane.

## Acknowledgment.

We are grateful to Prof. A.S.Arrott for helpful discussion. The work was supported by the RFBR (00-02-16485) and PSSNS Program grants.

## References

- [1] R.P.Cowburn, D.K.Koltsov, A.O.Adeyeye et al., Phys. Rev. Lett. **83**, 1042 (1999).
- [2] T.Shinjo, T.Okuno, R.Hassdorf et al., Science **289**, 930 (2000).
- [3] M.Schneider, H.Hoffmann, J.Zweck, Appl. Phys. Lett., **77**, 2909 (2000).
- [4] K.Bussmann et.al., J. Appl. Phys., **75**, 2476 (1999).
- [5] R.P.Cowburn, A.O.Adeyeye M.E.Welland. New Journal of Physics **1**, 16 (1999).
- [6] T.Tada and T.Kanayama, Jpn.J.Appl.Phys. **35**, L 63 (1996).
- [7] V.M.Mikushin, V.V.Shnitov, Fiz.Tverd.Tela., **39**, 187(1997) (in russian).

- [8] A. D.Kent et al. J.Appl.Phys. **67**, 6656 (1994).
- [9] V. M. Rosenbaum, Zh. Exp. Teor. Fiz., **99**, 1836 (1991) (in russian).
- [10] V. M. Rosenbaum, V. M. Ogenko, A. A. Chuiko, Uspekhi Fiz. Nauk, **161**, 79 (1991) (in russian).
- [11] R.P. Popko, L.L. Savchenko, N.V. Vorotnikov, Pis'ma JETP **69**, 555 (1999) (in russian).
- [12] E.D. Boerner, H.N. Bertran. IEEE Trans. on Magn. **33**, 3152 (1997).
- [13] to be published in Fizika Metallov i Metallovedenie (in russian)
- [14] R.P. Cowburn, M.E. Welland. Appl, Phys. Lett. **72**, 2041 (1998).
- [15] Y. Gaididei et al., Phys.Rev.B **59** 7010 (1999).